Runaway Phenomena in Low-Density Polyethylene Autoclave Reactors

Simon X. Zhang, Nolan K. Read, and W. Harmon Ray
Dept. of Chemical Engineering, University of Wisconsin—Madison, Madison, WI 53706

To study runaway behavior in autoclave low-density polyethylene (LDPE) reactors, a kinetic model for a perfectly stirred tank reactor is presented. The kinetic model not only includes the standard initiation, propagation, and termination reactions for polymerization, but it also has free radical reactions that describe the decomposition of ethylene ultimately leading to a runaway. Dynamic simulation of the model indicates runaway behavior for the following conditions: excess initiator in feed; feed impurity; feed temperature disturbance; controller failure; and poorly tuned controller. Operating strategies such as mixed initiator feeds and grade transitions are also explored from a dynamic view. Stability analysis indicates safe operating limits for certain variables at typical conditions. The model provides useful insights for preventing runaway reactions in LDPE autoclaves.

Introduction

Low-density polyethylene (LDPE) is a commodity polymer produced by free-radical polymerization at high pressure. Two types of processes are commonly used: a tubular process using a very long, small-diameter tubular reactor, and an autoclave process using a well-stirred tank reactor. The two processes enjoy equal popularity in industrial practice. Runaway reaction happens less frequently in tubular processes due to a higher cooling surface area. Thus this article will focus only on reactor runaway behavior in the autoclave process, a pernicious problem that has haunted LDPE producers since the beginning.

In roughly the same time period as the ICI researchers Fawcett and Gibson were discovering polyethylene in 1933 (Beasley, 1989), other researchers were discovering the explosive decomposition of ethylene at high pressure (Waterman and Tulleners, 1931; Egloff and Schaad, 1933). This decomposition is autoaccelerating because it is an exothermic reaction. Thus, while the high-pressure LDPE reactors can produce high volume and low-price products, there is an insidious threat of reactor runaway caused by the decomposition of ethylene.

Since decomposition or "decomp" occurs over a very small time interval, for example, one second (Huffman et al., 1974), there is no practical way to control the high temperature and pressure in the reactor once the decomp has started. Therefore, these reactors are equipped with relief valves that open at a specified upper pressure limit; the reactor contents, ethylene and by-products, then escape into the atmosphere where they self-ignite (Martinot, 1984) or are purposely ignited. Although the present focus is on decompositions in the LDPE reactor, mention should be made of decompositions in the product separator (Sullivan and Shannon, 1992), ethylene heater (Bowen, 1983), and pipe lines (McKay et al., 1977; Worrell, 1979). There are thus safety and environmental issues associated with this runaway problem.

Although there have been numerous publications on modeling LDPE autoclave and tubular reactors (Agrawal, 1975; Brandolin et al., 1988; Chan et al., 1993; Chen et al., 1976; Feucht et al., 1985; Goto et al., 1981; Hollar and Ehrlich, 1983; Marini and Georgakis, 1984a,b; Mavridis and Kiparissides, 1985; Shirodkar and Tsien, 1986; Zabisky et al., 1992), all these articles confine themselves to only polymerization and polymer molecular structure. With the exception of Gardner (1975) and Huffman et al. (1974) (linear dynamic analysis), no attempts have been made to include decomposition reactions even though experimental evidence indicates their importance. This exclusion severely limits the usefulness of the model in process synthesis, process optimization, and process control. This situation is, in part, due to the lack of a fundamental understanding of the decomposition. This work is the first to combine polymerization with decomposi-

Correspondence concerning this article should be addressed to W. H. Ray.
Present address of N. K. Read: DuPont Wash. Works, P.O. Box 1217, Parkersburg, WV 26102.

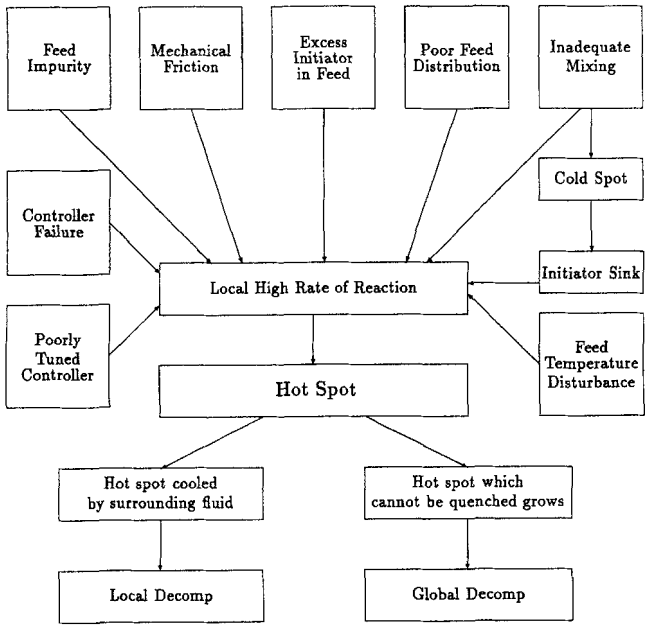

Figure 1. Possible explanations for the decomp.

All these phenomena tend to cause hot spots that ultimately could lead to decomp.

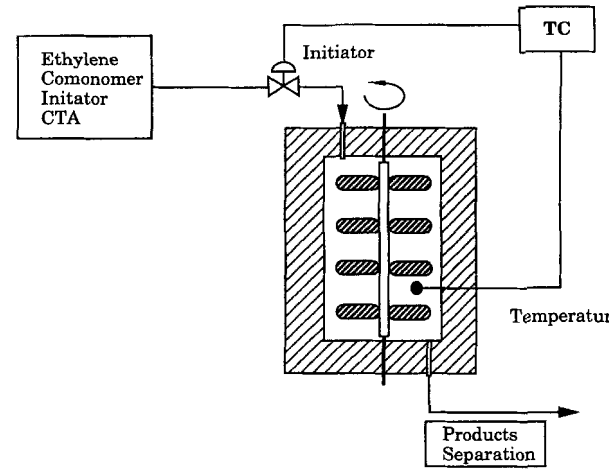

Figure 2. LDPE autoclave.

The autoclave represents a DuPont type with L/D ratio between 2 and 4. The reactor cooling is provided by cold, fresh feed, and the reactor temperature is regulated by initiator feed concentration.

tion in order to study the runaway behavior in a nonlinear dynamical framework.

It has been suggested that hot spots in the reactor initiate the runaway (Gardner, 1975). These hot spots can be caused by a number of incidents, some of which are listed in Figure 1. The goal of this article is to develop a kinetic and reactor model to elucidate the relationship between the incidents in Figure 1 and the eventual runaway or "decomp." In this article, we will address polymerization and decomposition in a perfectly mixed tank reactor. Decomposition due to feed impurity, feed temperature disturbance, excess initiator, controller failure, poorly tuned controller, or operating policy will be discussed. Examples with and without decomp will be compared. It is well known that in some cases LDPE autoclave reactors are imperfectly mixed. Decomposition in an imperfectly mixed reactor, such as by propagation of local hot spots, will be addressed in the upcoming articles.

Characteristics of the LDPE Autoclave

Some characteristics of the LDPE autoclave reactor (cf. Figure 2) that may contribute to runaway behavior are:

- The LDPE autoclave has very thick walls because the reactor is pressurized to around 2,000 atm (Christl and Roedel, 1959), so that the reactor can be viewed as an adiabatic reactor (Christl and Roedel, 1959; Tomura et al., 1978). This allows the adiabatic temperature rise to be used to calculate steady-state monomer conversion in good agreement with plant data (Tomura et al., 1978).
- The dependence of the reaction rate on temperature takes the Arrhenius form and provides good agreement between model results and experimental data (Chen et al., 1976; Goto et al., 1981; Verros et al., 1993). Thus the reactor system is highly nonlinear. Indeed, it has been found (Gardner, 1975; Hoftyzer and Zwietering, 1961) that up to five steady states exist in this system.
- Autocatalytic behavior of both the polymerization and decomposition make this reactor extremely sensitive to temperature disturbances.
- The temperature controller, which operates by manipulating the inlet initiator concentration, does not have much power in lowering high temperatures because the manipulated variable is constrained by a lower bound of zero. This discontinuity is an additional nonlinearity of the system. In addition, a disturbance (e.g., feed temperature) cannot be fully removed from the system because the compensation of the disturbance by manipulation of the inlet initiator concentration causes variability in the product properties.
- Most CSTR models (Chan et al., 1993; Gardner, 1975; Hoftyzer and Zwietering, 1961; Marini and Georgakis, 1984a) indicate an unstable operating point for the production of LDPE. One article (Marini and Georgakis, 1984a), though, indicates that imperfect mixing may actually stabilize the operating point.
- The LDPE reactor is operated at high temperatures and high pressures with vigorous mixing of reactants. The reaction temperature is sometimes close to the runaway boundary either locally or globally.
- The only cooling in this system comes from the cold inlet stream; in addition, the conversion is a function of this temperature difference. To obtain higher conversions, the steady-state temperature must be higher, indicating that the inlet stream must be colder to remove the excess heat. But increasing reactor temperature may move the reactor close to the unstable boundary.

Because of the design just described the LDPE reactor system is operated close to instability, sometimes leading to sudden runaway.

Thermal Decomposition of Ethylene

At high temperatures, 300–600°C, ethylene decomposes into hydrogen, carbon, methane, and by-products including

Table 1. Studies of Ethylene Decomposition

Products	Reference	Comments
C, CH_4, H_2, C_2H_2, C_4H_6	Towell and Martin, 1961	200–1,400°C, atmospheric pressure, H_2 dominant product with substantial amount of C present
C, CH_4, H_2, olefins	Egloff and Schaad, 1933	30–460°C, moderate pressure (50 atm); relative amounts of products not reported because autoclave leaked; only residual gas was analyzed
C, CH_4, H_2, C_2H_6, C_2H_2	Watanabe et al., 1972	100–1,500 atm, selectivity of products as function of temperature, C and CH_4 dominant products
C, CH_4, H_2	Gardner, 1975; Huffman et al., 1974	200–2,000°C, 1,400–7,000 atm, theoretical calculations conclude that C and CH_4, not H_2, are the dominant products
C, CH_4, H_2 C_2H_6	Scott et al., 1965	Near room temperature and 200–3,000 atm; report decomposition equation that shows dominant products are C and CH_4 with a small but significant amount of H_2
C, CH_4, H_2 C_6H_6	Waterman and Tulleners, 1931	20–400°C, 5–200 atm; mostly C, CH_4, some H_2
C, CH_4, H_2 C_6H_6	Britton et al., 1986	Discussed causes and prevention of ethylene decomposition; model proposed for pressure and temperature calculation
	Luft and Neumann, 1978; Neumann and Luft, 1973	40–330°C and 20–2,000 atm; decomp threshold temperature decreases with increasing pressure; maximum decomp pressure increases with initial density
C, gas not analyzed	Zimmermann and Luft, 1994; Bonsel and Luft, 1995	25–350°C and 500–4,000 atm; determined decomp limits under both local initiation and spontaneous thermal decomposition; measured decomp reaction rate

acetylene, ethane, and other low-saturated and unsaturated hydrocarbons (Laidler and Loucks, 1972; Hucknall, 1985; Miller, 1969; Tanzawa and Gardiner, 1980). At the high-pressure and high-temperature conditions of typical LDPE autoclave reactors, it is believed the dominant products are methane and carbon with a small but significant portion of hydrogen and possibly ethane. Any kinetic scheme that attempts to describe the decomposition must therefore account for the production of these products. Table 1 summarizes some important experimental and theoretical works on ethylene decomposition. Most of these studies start the decomposition with some ignition source or catalyst. These methods support the theory that hot spots are responsible for decomposition in LDPE autoclaves. The hot spots could be caused by mechanical friction (ignition source) and feed impurities such as acetylene (catalyst).

Decompositions are known to occur sporadically in LDPE autoclaves. The decomposition releases about 30.2 kcal/mol of heat. Because of the autoaccelerating and adiabatic nature of these reactors, once initiated these decompositions cause a runaway—with both a temperature and pressure spike—in a matter of seconds (Huffman et al., 1974; Iwasaki et al., 1987), that is, there is no time for the inlet flow to inhibit the runaway as long as the residence time of the reactor is on the order of 15 s to 2 min. These runaways cannot be predicted, and thus LDPE reactors are fitted with relief valves in order to vent the products of the decomposition and prevent the reactor from bursting.

Kinetics and Reactor Design

This kinetic scheme used here, Table 2, reflects the basic understanding of the initiation, propagation, and termination reactions of the polymerization, as well as a set of decomp reactions all taking place in a perfectly stirred tank reactor, Table 3. The goal here is to use these kinetics to develop an understanding of the runaway behavior in the LDPE system. The major attributes of this scheme include:

- The set of reactions for the polymerization represent the simplest scheme that retains the essential nonlinear kinetic behavior.
- The set of reactions presented for the decomp, although complex, seem to represent the available experimental data adequately (Watanabe et al., 1972). They are also consistent with the accepted free-radical path for decomposition (Laidler and Loucks, 1972; Benson and Haugen, 1967).
- The quasi-steady-state assumption for each of the radical concentrations is used.
- The decomp kinetics take the form presented by Watanabe et al. (1972) and predict the major products as C, CH_4, H_2, and C_2H_6, which is consistent with the experimental observations.
- The main sources of heat are the exothermic propagation and the decomposition of ethylene.
- This scheme ignores the production of higher olefins, which are small quantity by-products.
- There appear to be many kinetic parameters to choose in this decomp scheme. However, after proper simplification, there are only two independent parameters to be determined; they are determined from experimental observations.

Decomp kinetic scheme

A comprehensive ethylene decomposition kinetic scheme was proposed by Huffman et al. (1974). They also provided kinetic rate constants based on parameter values reported in the open literature. However, the rate constants for different kinetic steps were obtained from different authors, under different experimental conditions, and with different assumptions. As a result, the rate constants are not self-consistent

Table 2. Summary of Polymerization and Decomposition Kinetics*

Name	Reaction	Rate	Rate Using QSSA
		Polymerization	
Initiation	$I \rightarrow 2R\cdot$	$2fk_d[I]$	$2fk_d[I]$
Initiation	$2C_2H_2 \rightarrow 2R\cdot$	$2gk_a[C_2H_2]^2$	$2gk_a[C_2H_2]^2$
Propagation	$M + R\cdot \rightarrow R\cdot$	$k_p[M][R\cdot]$	$k_p[M]F^{**}$
Termination	$R\cdot + R\cdot \rightarrow P$	$k_{tt}[R\cdot]^2$	$k_{tt}F^2$
		Decomposition	
Initiation	$2M \rightarrow C_2H_3\cdot + C_2H_5\cdot$	$k_1[M]^2$	$k_1[M]^2$
Propagation	$C_2H_5\cdot \rightleftharpoons M + H\cdot$	$k_2[C_2H_5\cdot] - k_2'[M][H\cdot]$	$k_2A^{\dagger} - k_2'[M]D^{\ddagger}$
Propagation	$C_2H_5\cdot + M \rightarrow C_2H_6 + C_2H_3\cdot$	$k_3[C_2H_5\cdot][M]$	$k_3A[M]$
Propagation	$H\cdot + C_2H_4 \rightarrow H_2 + C_2H_3\cdot$	$k_4[H\cdot][M]$	$k_4D[M]$
Propagation	$C_2H_3\cdot \rightarrow C^{\S} + CH_3\cdot$	$k_5[C_2H_3\cdot]$	$k_5B^{\S}$
Propagation	$CH_3\cdot + C_2H_4 \rightarrow CH_4 + C_2H_3\cdot$	$k_6[CH_3\cdot][M]$	$k_6E^{\P}[M]$
Termination	$2CH_3\cdot \rightarrow C_2H_6$	$k_7[CH_3\cdot]^2$	$k^{\|}E^2$
Termination	$CH_3\cdot + C_2H_3\cdot \rightarrow C_2H_2 + CH_4$	$k_8[C_2H_3\cdot][CH_3\cdot]$	kBE
Termination	$2C_2H_3\cdot \rightarrow C_2H_2 + C_2H_4$	$k_9[C_2H_3\cdot]^2$	kB^2

*The decomposition scheme is due to Watanabe et al. (1972).

**$F = \left[\dfrac{fk_d[I] + gk_a[C_2H_2]^2}{k_{tc}}\right]^{1/2}$, the QSS concentration of free radicals formed by initiator and impurity.

†$A = \dfrac{k_1M^2(k_2' + k_4)}{k_2k_4 + k_3M(k_2' + k_4)}$, the QSS concentration of $C_2H_5\cdot$

‡$D = \dfrac{k_1k_2M}{k_2k_4 + k_2'k_3M + k_3k_4M}$, the QSS concentration of $H\cdot$

§$B = \dfrac{M}{2}\sqrt{\dfrac{2k_1}{k}}$, the QSS concentration of $C_2H_3\cdot$

¶$E = \dfrac{M}{2}\sqrt{\dfrac{2k_1}{k}}$, the QSS concentration of $CH_3\cdot$

‖$k = k_7 = k_8 = k_9$, assumption of equal termination rate constants.

within the proposed kinetic scheme. Initial attempts to use Huffman's kinetic scheme and parameters were not successful in representing the experimental observations of ethylene decomposition. Because there are many independent parameters to be determined for the full decomp model and there are few experimental results available in the literature, it is not possible to determine all the rate constants from experimental data.

For these reasons, a simplified decomp kinetic scheme with a minimum number of independent kinetic parameters is used. The simplified ethylene decomp kinetic scheme is presented in Table 4. This kinetic scheme includes the important kinetic mechanisms that produce the major decomp products and is based on the scheme originally proposed by Watanabe et al. (1972).

Even with the simplified decomp kinetic scheme, there are still many rate constants that need to be determined before the decomp model can be used for simulation. However, there is not a consistent set of kinetic rate constants available in the literature, and the data from different sources have significant inconsistencies. Thus, it is necessary to further simplify the decomp kinetic scheme and reduce the number of independent parameters.

There are four radicals involved in our simplified ethylene decomp kinetic scheme, $C_2H_5\cdot$, $C_2H_3\cdot$, $CH_3\cdot$ and $H\cdot$. They can be expressed in analytical form by assuming the quasi-steady-state assumption (QSSA) for their respective balance equations.

$$\frac{d[C_2H_5\cdot]}{dt} = k_1[M]^2 - k_2[C_2H_5\cdot] + k_2'[M][H\cdot] - k_3[M][C_2H_5\cdot] \quad (1)$$

Table 3. Reactor Design and Operation

Variable	Symbol	Value
Volume	V	1,000 L
Residence Time	τ	75 s
Reactor Pressure	P	2,000 atm
Feed Conc. of Initiator	c_{If}	7.5 ppm
Feed Temperature	T_f	120°C
Exit Temperature	T_0	239°C
Monomer Conversion	X_p	0.106

Table 4. Ethylene Decomposition Kinetic Scheme

Initiation:	$2\,C_2H_4 \xrightarrow{k_1} C_2H_3\cdot + C_2H_5\cdot$
Propagation:	$C_2H_5\cdot \xleftrightarrow{k_2,k_2'} C_2H_4 + H\cdot$
	$C_2H_5\cdot + C_2H_4 \xrightarrow{k_3} C_2H_6 + C_2H_3\cdot$
	$H\cdot + C_2H_4 \xrightarrow{k_4} H_2 + C_2H_3\cdot$
	$C_2H_3\cdot \xrightarrow{k_5} C + CH_3\cdot$
	$CH_3\cdot + C_2H_4 \xrightarrow{k_6} CH_4 + C_2H_3\cdot$
Termination:	$CH_3\cdot + CH_3\cdot \xrightarrow{k_7} C_2H_6$
	$C_2H_3\cdot + CH_3\cdot \xrightarrow{k_8} C_2H_2 + CH_4$
	$C_2H_3\cdot + C_2H_3\cdot \xrightarrow{k_9} C_2H_2 + C_2H_4$

$$\frac{d[C_2H_3\cdot]}{dt} = k_1[M]^2 + k_3[M][C_2H_5\cdot] + k_4[M][H\cdot] - k_5[C_2H_3\cdot] + k_6[M][CH_3\cdot] - k_8[C_2H_3\cdot][CH_3\cdot] - k_9[C_2H_3\cdot]^2 \quad (2)$$

$$\frac{d[CH_3\cdot]}{dt} = k_5[C_2H_3\cdot] - k_6[M][CH_3\cdot] - k_7[CH_3\cdot]^2 - k_8[C_2H_3\cdot][CH_3\cdot] \quad (3)$$

$$\frac{d[H\cdot]}{dt} = k_2[C_2H_5\cdot] - k'_2[M][CH_3\cdot] - k_4[H\cdot]. \quad (4)$$

From Eqs. 1 and 4, $[C_2H_5\cdot]$ and $[H\cdot]$ are given by

$$[C_2H_5\cdot] = \frac{k_1[M]^2(k'_2 + k_4)}{k_2k_4 + k'_2k_3[M] + k_3k_4[M]} \quad (5)$$

$$[H\cdot] = \frac{k_1k_2[M]}{k_2k_4 + k'_2k_3[M] + k_3k_4[M]}. \quad (6)$$

Following Watanabe et al. (1972), if the termination rate constants k_7, k_8, and k_9 are assumed to have the equal value k_t, Eqs. 2 and 3 can be simplified as

$$2k_1[M]^2 - k_t([C_2H_3\cdot] + [CH_3\cdot])^2 = 0. \quad (7)$$

Since C and CH_4 are the dominant decomp products, the kinetic steps producing them should be the dominant kinetic steps. Further, assuming $[C_2H_3\cdot]$ and $[CH_3\cdot]$ to have equal values, the preceding equation becomes

$$[C_2H_3\cdot] = [CH_3\cdot] = \frac{[M]}{2}\sqrt{\frac{2k_1}{k_t}}. \quad (8)$$

The rates of generation of decomp products are then given by the following equations:

$$\frac{d[C]}{dt} = k_5[C_2H_3\cdot] = \frac{k_6}{2}\sqrt{\frac{2k_1}{k_t}}[M]^2 \quad (9)$$

$$\frac{d[CH_4]}{dt} = k_6[M][CH_3\cdot] + k_8[C_2H_3\cdot][CH_3\cdot] = \left(\frac{k_1}{2} + \frac{k_6}{2}\sqrt{\frac{2k_1}{k_t}}\right)[M]^2 \quad (10)$$

$$\frac{d[C_2H_6]}{dt} = k_3[M][C_2H_5\cdot] + k_7[CH_3\cdot]^2 = \frac{3}{2}k_1[M]^2 \quad (11)$$

$$\frac{d[C_2H_2]}{dt} = k_3[C_2H_3\cdot][CH_3\cdot] + k_9[C_2H_3\cdot]^2 = k_1[M]^2. \quad (12)$$

Thus, the decomp products generation rates consist of two parts: $k_1[M]^2$, corresponding to ethylene decomposition into radicals, and $k_6/2\sqrt{(2k_1/k_t)}$ $[M]^2$, representing the consumption of ethylene through propagation steps. With the simplified decomp scheme, there are only two independent rate constants that need to be determined: k_1 and $k_6k_t^{-0.5}$. They can be determined from two pieces of information: the crossing temperature of the decomp reaction rate with the polymerization rate and the decomp products distribution at a specified temperature. In this article, the crossing temperature is chosen to be 310°C. This choice is based on the fact that the decomp reaction happens at about 330°C when catalyst exists and about 400°C without catalyst (Waterman and Tulleners, 1931). The decomp product distributions are based on the average of the experimental results of Watanabe et al. (1972).

Polymerization kinetics

The general kinetic scheme of free-radical polymerization has been proposed for both homopolymerization and copolymerization (Arriola, 1989). This scheme allows the prediction of polymer chain-length distributions as well as copolymer composition and sequence chain length. Since under the possible decomp conditions, polymer products' molecular structure, such as molecular weight distribution and copolymer composition, becomes of less importance than the issue of reactor safety, only the kinetic steps that influence monomer conversion and heat of reaction are included in the decomp model. These reactions include initiation by initiator and impurity, propagation, and chain termination. Table 5 shows the simplified free-radical polymerization kinetic scheme. In the table, $D_{n,b}$ refers to dead polymer with chain length n and trifunctional branching points b; $P_{i,n,b}$ represents the live polymer with chain length n, trifunctional branching points b, and end group of type i. The kinetic parameters for polymerization and decomposition reactions are listed in Table 6.

Material and energy balances

The reactor model assumes a well-mixed tank reactor with multiple inlet and outlet streams available. The model is written in a very general way such that different reaction media, outflow types, and thermal conditions can be modeled as special cases of the general model. The balance equations of the tank reactor include:

- Material balances for monomer, polymer, decomp products, and other nonpolymer species.

Table 5. Simplified Kinetics of Free-Radical Polymerization

Initiation:	
Peroxide or azo-compound decomposition	$I \xrightarrow{fk_d} 2R\cdot$ $R\cdot \xrightarrow{\text{fast}} P_{1,0}$
Special Initiation:	$C + M \xrightarrow{gk_i} P_{1,0}$
Propagation:	
Forward and reverse	$P_{n,b} + M \xleftrightarrow{k_p} P_{n+1,b}$
Termination:	
By coupling	$P_{n,b} + P_{m,c} \xrightarrow{k_{tc}} D_{n+m,b+c}$
By disproportionation	$P_{n,b} + P_{m,c} \xrightarrow{k_{td}} D_{n,b} + D_{m,c}$
By inhibition	$P_{n,b} + X \xrightarrow{k_{tx}} D_{n,b}$
Spontaneous	$P_{n,b} \xrightarrow{k_{tsp}} D_{n,b}$

Table 6. Kinetic Parameters*

Reaction	k_0 (1/mol·s)	E_a (cal/mol)	V_a^{**} (cal/atm·mol)	Reference
DTBP k_{d1}	1.81×10^{16}	38,400	0.0605	Chen et al., 1976
TBPA k_{d2}	2.83×10^{15}	34,584	0.0605	Doak, 1986
Acetylene k_{d3}	2.944×10^{10}	16,828	0.0	Gay et al., 1965
k_p	1.14×10^{7}	7,091	−0.477	Chen et al., 1976
k_{tc}	3.00×10^{9}	2,400	0.3147	Chen et al., 1976
k_1	4.003×10^{19}	65,000	−0.1937	This work
$k_6k_t^{-0.5}$	1.587×10^{20}	65,000	0.32185	This work
ΔH_{poly}	−24,000 (cal/gmol)			Chen et al., 1976
ΔH_{decomp}	−30,200 (cal/gmol)			Huffman et al., 1974

*Rate constants are expressed in generalized Arrhenius form ($k = k_0\exp(-(E_a + V_aP)/RT)$).
**V_a can be expressed in cm^3 by using conversion factor 41.293.

• An energy balance for the continuous tank reactor.

Physical Properties. The reactor contents are treated as a single-phase mixture with only monomer, polymer, solvent (here monomer), and decomp products considered to have significant volume. Other species, such as initiator, impurity, and inhibitor, exist only in trace amounts and have negligible volume contribution.

Component densities and heat capacities are polynomial functions of reactor temperature and pressure.

$$\rho_i = \rho_{i0} + \sum_{k=1}^{3} c_{ik}T^k + \sum_{k=1}^{3} d_{ik}P^k \tag{13}$$

$$C_{p_i} = C_{p_{i0}} + b_{i_1}T. \tag{14}$$

The reacting mixture properties are calculated from the individual component physical properties assuming volume additivity

$$\frac{1}{\rho} = \sum_{k=1}^{N} \frac{W_k}{\rho_k} \tag{15}$$

$$C_p = \sum_{k=1}^{N} W_k C_{pk}, \tag{16}$$

where N is number of components with significant volume contributions.

Material Balance. A total material balance around the well-mixed reactor yields

$$\frac{d(V\rho)}{dt} = Q^{in}\rho^{in} - Q\rho, \tag{17}$$

where ρ is the density of reacting mixture at the reactor temperature, pressure, and mixture composition. Assuming volume additivity of all the components having significant volume, the total material balance becomes

$$Q + \frac{dV}{dt} = \frac{Q^{in}\rho^{in}}{\rho} - V\rho\frac{dP}{dt}\sum_{i=1}^{N_{sp}}\frac{w_i}{\rho_i^2}\frac{d\rho_i}{dP} + V\rho\sum_{i=1}^{N_{sp}}\frac{1}{\rho_i}\frac{dw_i}{dt} - V\rho\frac{dT}{dt}\sum_{i=1}^{N_{sp}}\frac{w_i}{\rho_i^2}\frac{d\rho_i}{dT}. \tag{18}$$

The fraction monomer conversion X_p is defined as the fraction of monomer units being converted into polymer over the total amount of monomer units in the reactor, which includes both monomers and polymers:

$$X_p = \frac{[P]}{[M]+[P]}. \tag{19}$$

The balance equation for monomer conversion in a CSTR is

$$\frac{d\left[V\rho\left(1-W_S-\Sigma_{i=1}^{N}W_{D_i}\right)(1-X_p)\right]}{dt} = Q^{in}\rho^{in}\left(1-W_S^{in}-\sum_{i=1}^{N}W_{D_i}^{in}\right)\left(1-X_p^{in}\right) - Q\rho\left(1-W_S-\sum_{i=1}^{N}W_{D_i}\right)(1-X_p) - VMW_MR_P. \tag{20}$$

The balance equations for nonpolymer species in the tank reactor are given by:

• Initiator

$$\frac{dW_I}{dt} = \frac{Q^{in}\rho^{in}}{V\rho}(W_I^{in} - W_I) - fk_dW_I. \tag{21}$$

• Solvent

$$\frac{dW_S}{dt} \simeq \frac{Q^{in}\rho^{in}}{V\rho}(W_S^{in} - W_S). \tag{22}$$

• Decomp products

$$\frac{dW_{D_i}}{dt} = \frac{Q^{in}\rho^{in}}{V\rho}\left(W_{D_i}^{in} - W_{D_i}\right) - R_{W_{D_i}}^{k}. \tag{23}$$

• Inhibitor

$$\frac{dW_X}{dt} = \frac{Q^{in}\rho^{in}}{V\rho}(W_X^{in} - W_X) - k_{tx}W_X[R]. \tag{24}$$

Energy Balance. The generalized total energy balance around the well-mixed tank reactor is

$$\frac{d(V\rho e)}{dt} + c\frac{dT}{dt} = -Q^{in}\rho^{in}e^{in} - Q\rho e + E_{\text{input}} + V(R_p\Delta H_{poly} + R_d\Delta H_{\text{decomp}}), \quad (25)$$

where c is the reactor wall heat capacity and e is the enthalpy of reaction mixture per unit mass:

$$e = \int_{T_{\text{ref}}}^{T} c_p dT \quad (26)$$

Controller design

As is common in industrial LDPE reactors (Gemassmer, 1978), a feedback controller is used to regulate reactor temperature by manipulating the inlet concentration of initiator. As mentioned in Gemassmer (1978), there also may be a pressure controller on this reactor manipulating the outlet flow to keep the pressure at its set point. Although the pressure control is important, in the model presented here, pressure is assumed constant until a temperature runaway occurs, at which time a decomp is assumed and the simulation ended.

Commonly, LDPE operation at high temperatures has only a small stable region without feedback control. In this article, though, a high-temperature stable operating point was found. This enabled a linear-process model, valid only in a small region around the operating point, to be identified via an open-loop step input change. The process model in the Laplace domain is

$$y(s) = \frac{5.16\times10^{6}}{457s+1}u(s), \quad (27)$$

where $y(s)$ is the output (temperature deviation), $u(s)$ is the input (initiator feed rate), and s is a complex variable. The gain is very large, mainly because the manipulated variable is in parts per million (ppm) by weight concentration. The other variable of concern is the time constant, which is very large (457 s). As mentioned before, runaways in this reactor happen in approximately one second. Thus, this "sluggish" time constant is a possible source of problems.

Because the model has no time delay, conventional tuning methods such as Ziegler–Nichols cannot be used. Therefore, the controller parameters are obtained from dynamic simulation with the linearized model (Eq. 27). The controller is tuned so that there is a quick rise to the set point with very little overshoot. The following controller constants are obtained

$$K_c = 1.0\times10^{-6}, \qquad \frac{1}{\tau_I} = 1.0\times10^{-2} \quad (28)$$

for the continuous PI controller. For the P controller, K_c will be the same as Eq. 28. The closed-loop under P control is not as effective as the PI control, as it exhibits offset. Nevertheless, the controlled response was deemed adequate. The PI controller setting will produce a closed-loop response that has some overshoot with very rapid setpoint tracking.

Reactor design

The reactor studied is a perfectly mixed continuous stirred-tank reactor (CSTR). The reactor is operated in adiabatic mode, with cooling provided solely by cold, fresh feed. A feedback P or PI controller is used to regulate reactor temperature by manipulating the initiator feed concentration. The reactor design and operating parameters represent typical values encountered in industrial practice (Table 3).

Numerical Solution

The material and energy balances and equations resulting from recycle streams are represented by a set of differential and algebraic equations (DAEs). These equations, which can be written as

$$f(x,\dot{x},\theta,t) = 0 \quad (29)$$

implicitly describe the relationship between the state, x, time derivative of the state, $\dot{x}$, model parameters, θ, and time, t. The full set of modeling equations is solved simultaneously by the differential–algebraic system solver DASSL (Petzold, 1982) for dynamic simulation and by a modified version of the general continuation package AUTO (Doedel, 1986). Because of the DAE formulation of the process models, major modifications of AUTO were required, since AUTO was designed for differential equations. Detailed discussion of modifications made to AUTO are presented in other articles (Hyanek et al., 1995; Zacca et al., 1995).

Results and Discussion

The simulation results consist of two parts: the transient solution and the steady-state solution. LDPE model simulation to obtain the transient solution is common (Chan et al., 1993), the difference here being the inclusion of the decomposition kinetics, which yields a more realistic representation. In this section, dynamic responses for the LDPE reactor are given for certain disturbances.

Continuation analysis of the reactor offers important information regarding possible steady states and their stability. Many articles are published on continuation analysis of the LDPE autoclave (Gardner, 1975; Hoftyzer and Zwietering, 1961). However, all of them included only polymerization in their models, which significantly limited the predictive power of their respective models. In this section, some continuation analyses on important operating parameters are presented including both polymerization and decomposition kinetics.

Decomposition and polymerization

It is important to know the relative magnitudes of the polymerization and decomposition rates at different temperatures since ethylene is found to undergo polymerization at typical operating temperatures (below 300°C) but tends to decompose at elevated temperatures (Bonsel and Luft, 1995). Figure 3 illustrates the polymerization and decomposition rates of ethylene as a function of temperature. Polymerization dominates in the low-temperature range and decomposition takes over at higher temperatures. The two reaction rates cross at about 310°C; it is generally accepted that above 300°C there is threat of decomposition (Marini and Georgakis,

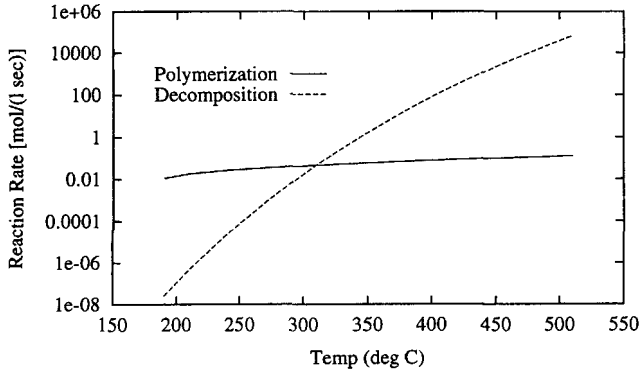

Figure 3. Polymerization and decomposition rates.

Polymerization and decomposition rates of ethylene are shown as functions of temperature. At typical operating temperatures, polymerization dominates; at elevated temperatures (above 310°C), decomposition of ethylene dominates.

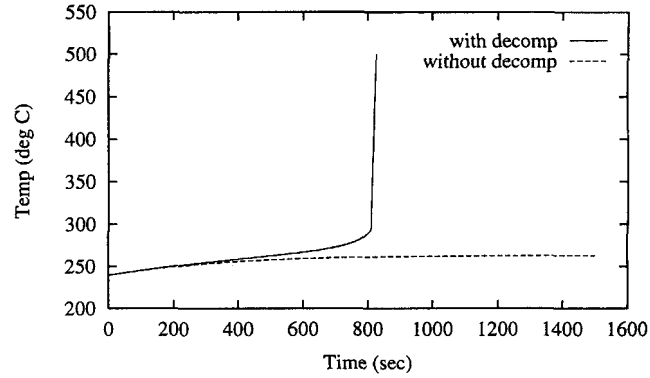

Figure 5. Reactor dynamics with and without the decomp reaction.

Dynamic responses of the LDPE autoclave to a feed disturbance with and without decomposition reactions are shown. The disturbance is a step change in initiator concentration from 7.3 ppm to 8.0 ppm.

1984a; Bonsel and Luft, 1995) so the crossover of 310°C is reasonable. So if the reactor can be kept below a certain critical temperature, the decomp can, in principle, be avoided. However, as is shown later, it is not easy to maintain a steady reaction temperature due to a fast reaction rate, a short residence time, and no external cooling. Local areas of high temperature or hot spots can also be caused by imperfect mixing and can propagate through the reactor and result in a global decomp.

Figure 4 compares the consumption rate of ethylene and the generation rate of decomp products as functions of ethylene fugacity at 410°C. The results from the present model are compared with the experimental results from Watanabe et al. (1972), and good agreement is observed. The normalized reaction rates for ethylene, methane, carbon, and ethane are proportional to the square of ethylene fugacity, indicating an apparent second-order reaction rate with respect to ethylene concentration. This is consistent with our proposed kinetic scheme (Eqs. 9–12).

Figure 5 shows the open-loop response of the LDPE reactor when subjected to a step increase in initiator feed concentration from 7.3 ppm to 8.0 ppm. When only the ethylene polymerization is included, reactor temperature increases slightly to about 250°C and settles down at a new steady state; there is no reactor runaway. However, if both decomp and polymerization schemes are included in the model, a 0.7-ppm

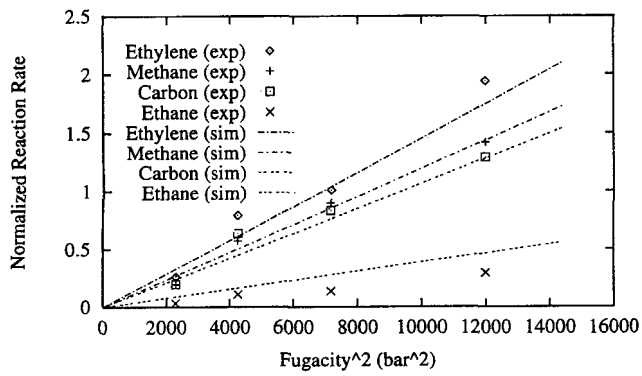

Figure 4. Comparison with decomp experimental results.

The consumption rate of ethylene and the production rate of decomp products as functions of ethylene fugacity are compared with experimental results from Watanabe et al. (1972). The reaction rate is normalized with respect to the production rate of carbon at a fugacity of 109.5 bar.

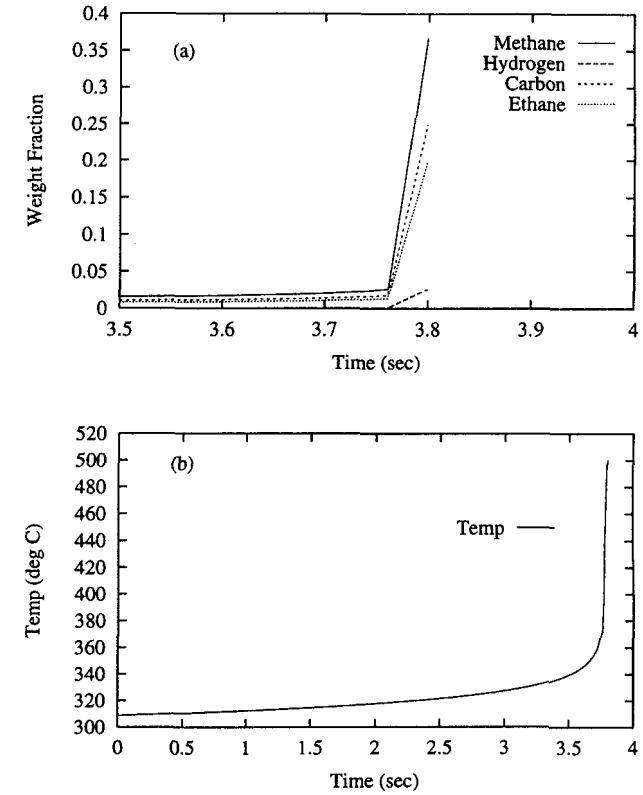

Figure 6. Decomp product distribution.

(a) Decomp product distribution during a runaway reaction in an LDPE autoclave. The decomp products' distribution is in good agreement with experimental observations (Watanabe et al., 1972). Methane, carbon, and hydrogen are the major decomp products with a minor amount of ethane. (b) The corresponding temperature response during the decomp.

increase in the initiator feed will eventually lead to a reactor runaway. This result suggests that the LDPE autoclave is operated close to instability. Some kind of control strategy is needed for stable and safe operation.

Decomp products distribution

Figure 6 shows the major decomp products distribution during a decomposition or runaway in an LDPE autoclave. Methane, carbon, and hydrogen are the major decomp products with a minor amount of C_2H_6. The decomp products distribution predicted by the model is in good agreement with experimental observations (Watanabe et al., 1972). The dramatic temperature increase happens in a few seconds during the runaway, which is also consistent with experiments.

Inlet initiator concentration

Figure 7 compares the reactor steady-state temperature as a function of inlet initiator concentration with and without decomp kinetics in the model; the initiator is di-*tert*-butyl peroxide (DTBP). When the decomp reactions are not included in the model, the temperature continuation diagram has the typical sigmoidal shape, which is similar to the one commonly encountered in a nonisothermal CSTR. However, the upper branch of the continuation diagram is completely different once the decomp reactions are included. The upper unstable branch with decomposition reaction included increases in temperature with decreasing inlet initiator concentration. At high temperatures, the ethylene starts to decompose and the decomp reactions overcome the polymerization reactions to become the dominant reaction path; there appears an upper stable steady state. With ample amount of monomer available for decomposing into free radicals, there is no need for additional initiator to sustain the high-temperature steady state. The upper steady state of 2,200°C is calculated from the adiabatic temperature rise corresponding to complete ethylene decomposition.

Based on the continuation diagram, it would be impossible to try to operate above 300°C at 75-s residence time even with a controller, since the typical controller manipulated variable is initiator feed concentration. Once a decomp happens, the controller is shut off because the decomp reaction does not need any more initiator to proceed. However, the opposite conclusion would be drawn if only polymerization is included in the model. This result suggests the importance of considering both decomp and polymerization kinetics in doing process analysis, design, and control.

In LDPE production, different initiators are used, depending on the reactor operating temperature (Luft et al., 1977). A more reactive ("fast") initiator is generally used at low temperatures, while a less reactive ("slow") initiator is used at high temperatures. Figure 8 compares the steady-state temperature for a faster initiator, *t*-butyl peroxyacetate

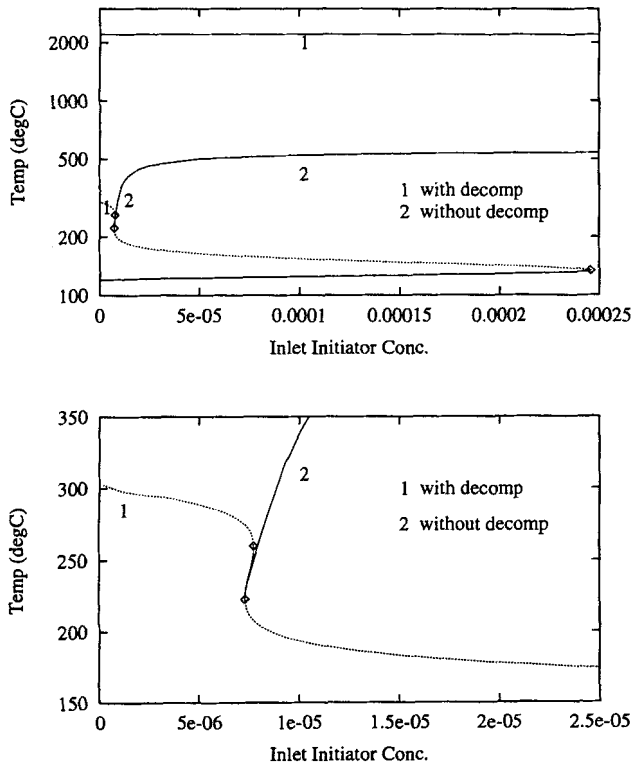

Figure 7. Continuation diagram of reactor temperature vs. initiator feed concentration.

The steady-state reactor temperature is shown as a function of initiator feed concentration with either decomp or nondecomp kinetics in the model. The upper stable branch with decomp corresponds to the adiabatic temperature rise from complete decomposition.

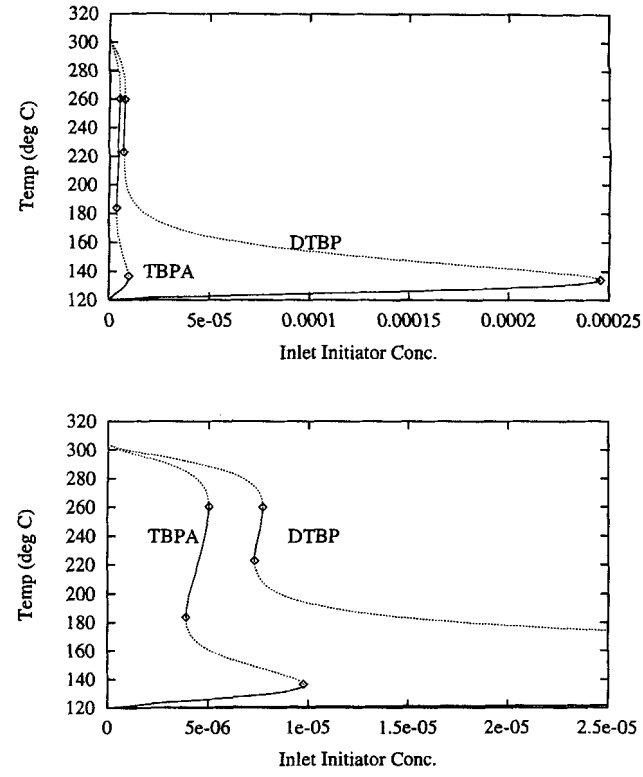

Figure 8. Continuation diagram of temperature vs. inlet initiator concentration for initiators with different decomposition rates.

The steady-state reactor temperature is shown as a function of initiator feed concentration with decomp kinetics included. The second initiator used is *t*-butyl peroxyacetate (TBPA), which has a much faster decomposition rate than DTBP. The reactor inlet temperature and ethylene feed flow rate are the same for the two different initiators.

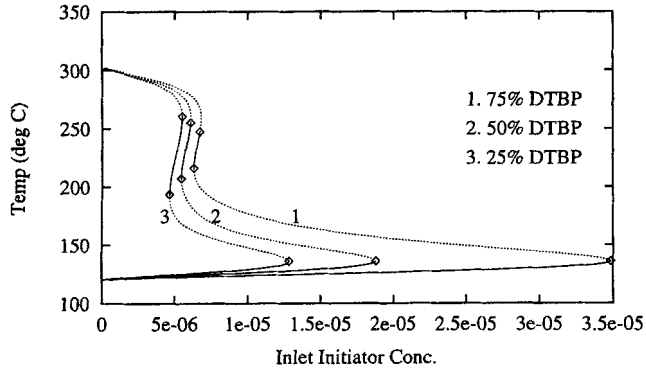

Figure 9. Continuation diagram of mixed initiator.

Steady-state reactor temperature is shown as a function of total initiator feed concentration. The initiator used is a mixture of high-temperature initiator DTBP and low-temperature initiator TBPA.

(TBPA), with a slower initiator, DTBP. Since the useful operating temperature is generally near the branch of upper steady states, it is important to know the stability of these steady states. The faster initiator (TBPA) tends to have a wider range of stable steady-state temperatures; the slower initiator (DTBP) has wider range of low-temperature steady states, but narrower range of upper steady states because of the decomp reactions. When the temperature is above 280°C, the steady states of both initiators approach each other and move toward zero initiator concentration, indicating the onset of decomp reactions. At this point ethylene decomposition overtakes polymerization as the dominant mechanism.

In many industrial reactors, there are temperature variations inside the reactor. A mixture of initiators with different decomposing rates is often used to optimize reactor productivity. Depending upon the composition of the initiator mixture, the reactor steady states and stability will be different. Figure 9 follows the steady-state temperature as a function of total inlet initiator concentration for mixtures of TBPA and DTBP. As the fraction of slow initiator (DTBP) increases, the lower stable steady-state temperature moves toward higher initiator concentration; the range of the upper stable steady state decreases.

Feed impurity

Small amounts of impurities (e.g., acetylene) can be found in the reactor feed; they can decompose into free radicals and induce runaway reactions. Figure 10 shows the influence of inlet acetylene concentration on the steady-state temperature under both open- and closed-loop conditions. Without a controller, very small amounts of acetylene can cause reactor runaway; but with just a simple P controller, steady-state operation can be achieved even at a much higher acetylene concentration. This prediction is confirmed by the dynamic response of the system as shown in Figure 11. In the closed-loop

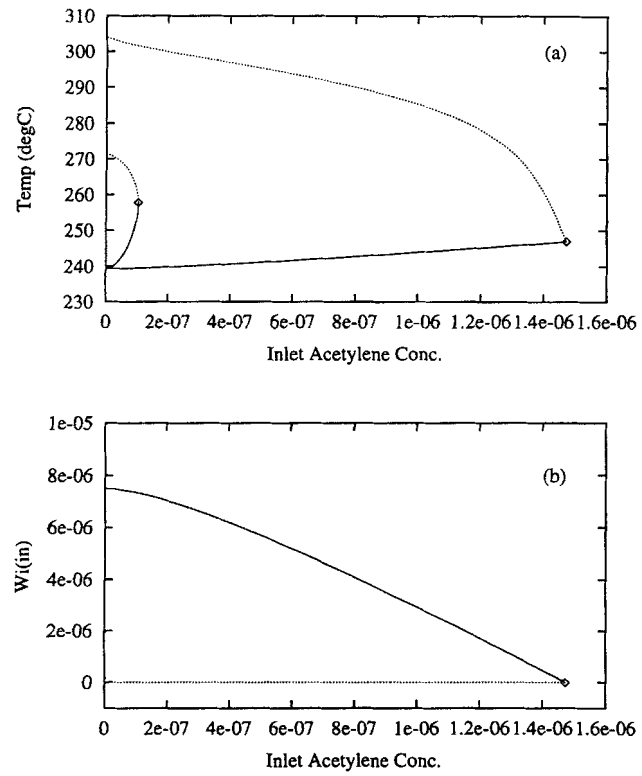

Figure 10. Continuation diagram of reactor temperature vs. impurity concentration.

(a) The steady-state reactor temperature is shown as a function of inlet acetylene concentration under both open-loop and closed-loop conditions. The controller is a proportional controller. (b) The controller action is shown as a function of feed impurity.

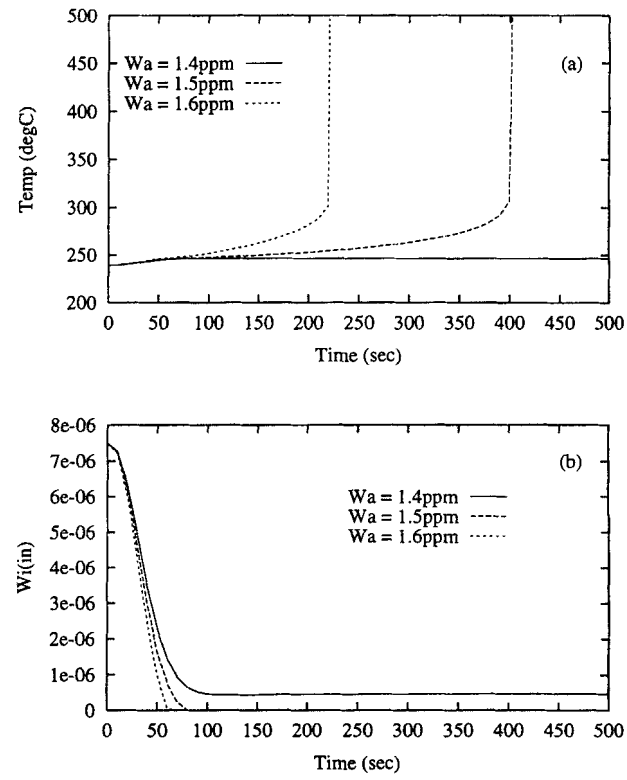

Figure 11. Effect of feed impurity.

(a) Closed-loop temperature responses to different acetylene levels in the feed. The reactor is under *P* control. (b) Responses of the manipulated variable, initiator feed, to the acetylene disturbance.

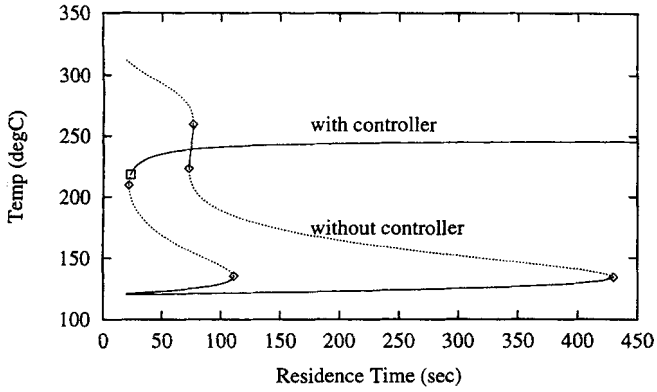

Figure 12. Continuation diagram of reactor temperature vs. reactor residence time.

The steady-state reactor temperature is shown as a function of residence time with decomp reactions included. The initiator used is DTBP, and the figure shows the behavior of the LDPE system with and without the *P*-controller.

simulation, the reactor temperature is controlled by manipulating the initiator feed concentration. With only a slight change in acetylene concentration, the reactor temperature changes from stable operation to runaway.

Residence time

Due to high reaction rates and limited cooling capacity, LDPE autoclaves usually have very short residence times, ranging from 15 s to 2 min (Gemassmer, 1978). Since the reactor operates in an adiabatic mode and the only cooling is fresh, cold monomer feed, it is important to study the effects of residence time on reactor stability. Figure 12 shows the influence of residence time on steady-state temperature under both open and closed-loop conditions. Under open-loop conditions, the high-temperature stable steady states only exist over a narrow residence time range; but once a controller is used, the reactor can operate with stability at high temperature over a wide residence time range.

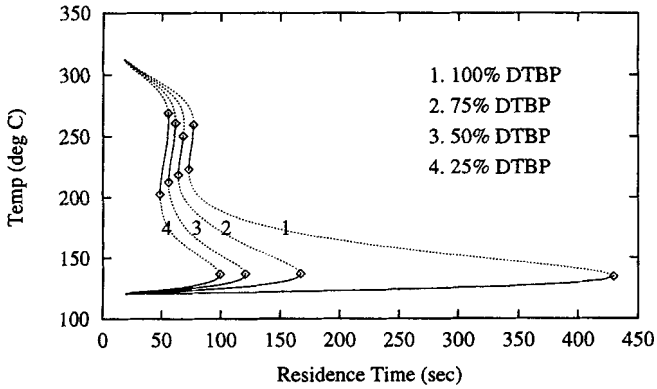

Figure 13. Effect of residence time with mixed initiators.

The steady-state reactor temperature is shown as a function of residence time at different mixed initiator compositions. The initiator used is a mixture of DTBP and TBPA. The total initiator feed concentration is the same for different initiator mixture compositions.

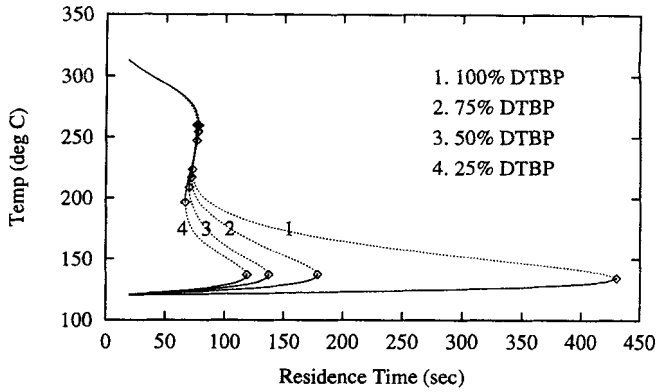

Figure 14. Effect of residence time with mixed initiators.

The steady-state reactor temperature is shown as a function of residence time at different mixed initiator compositions. The initiator used is a mixture of DTBP and TBPA. The total initiator feed concentrations are optimized for different initiator mixture compositions to maintain the same outlet temperature, $T = 239°C$, at 75 s residence time.

Figure 13 shows the effect of residence time when a mixture of two different initiators is used. The total initiator feed concentration is kept the same while composition of the mixture changes. As the fraction of slow initiator (DTBP) increases, the upper stable steady state moves toward higher residence time, while the stable upper temperature decreases with increasing DTBP fraction. At very high temperatures, all the curves merge together as the decomp reactions take over.

If the reactor outlet temperature needs to be fixed at a certain residence time, then the total initiator feed has to be changed, keeping the same initiator mixture composition. Figure 14 presents the case where the outlet temperature at 75-s residence time is the same at different initiator mixture compositions. The general trend of the curves is similar to Figure 13, but the upper steady states are almost the same with different initiator compositions.

Feed temperature

Feed temperature is an important parameter in LDPE autoclave operation since the reactor operates adiabatically and the cold, fresh feed is the sole source of reactor cooling. As a result, a small variation in feed temperature may potentially cause a reactor runaway. Figure 15 shows the reactor steady-state temperature as a function of feed temperature for DTBP and an equal-by-weight mixture of DTBP and TBPA. The inlet flow rate and total initiator concentration are kept the same for both cases. For both types of initiators, the reactor is unstable over a wide range of feed temperature. For the slow initiator DTBP, the upper stable branch exists at a higher feed temperature than when a mixture of DTBP and TBPA is used. For both initiators, the lower steady states have a similar inlet and outlet temperature, indicating reaction extinction.

Figure 16 is similar to Figure 15 except that the total initiator feed concentrations are optimized to maintain the same exit temperature when the feed temperature is 120°C. Both initiators seem to have the same unstable upper branches,

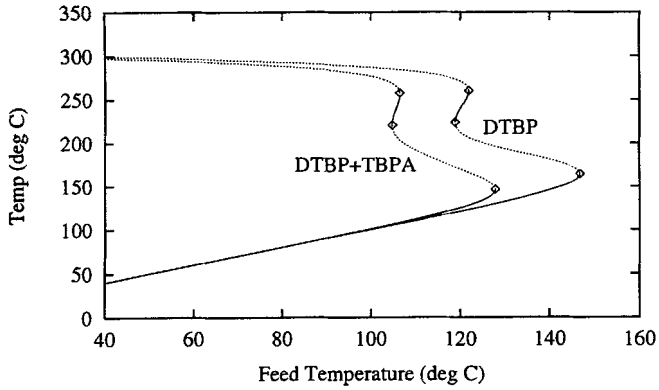

Figure 15. Continuation diagram of reactor temperature vs. inlet temperature.

Steady-state reactor temperature is shown as a function of inlet temperature with decomp reactions included. Two kinds of initiators are used, DTBP and an equal-by-weight mixture of DTBP and TBPA. The total initiator feed concentrations are the same for both cases.

while the DTBP and TBPA mixture has a wider upper stable temperature range than with DTBP alone. On the other hand, DTBP has wider low steady-state range.

From Figure 16, if DTBP is the only initiator used, the reactor will be open-loop stable at 121°C feed temperature, but unstable when feed temperature is above 125°C. Figure 17 confirms this conclusion. The reactor is able to reach a new steady state when there is a step increase in feed temperature to 121°C, but has a runaway reaction if the feed temperature is changed to 125°C or 130°C.

Feed temperature may also affect the reactor stability when there is an impurity in the feed stream. Figure 18 shows the dynamics at different feed temperatures when the system is subjected to a sudden impurity feed disturbance. If the feed temperature is 120°C, the system will be unstable based on the continuation diagram in Figure 10. The dynamic simulation shows that a runaway reaction happens as a result of a 2-ppm acetylene disturbance. However, if the feed temperature is lowered to 80°C, the system reaches a new steady state with the 2-ppm acetylene disturbance. This indicates that a reactor operating at lower inlet temperature can sustain a higher impurity level.

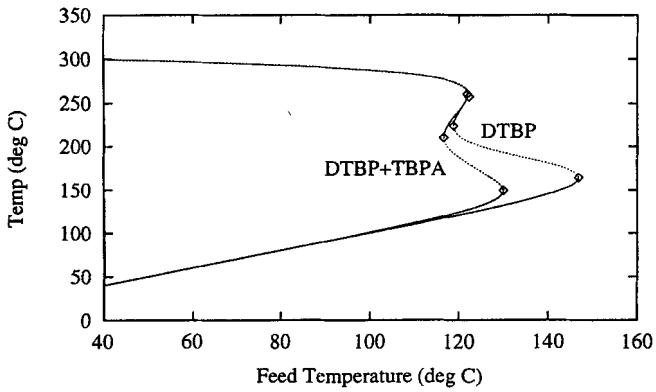

Figure 16. Continuation diagram of reactor temperature vs. inlet temperature.

Steady-state reactor temperature is shown as a function of inlet temperature with decomp reactions included. Two kinds of initiators are used, DTBP and an equal-by-weight mixture of DTBP and TBPA. The total initiator feed concentrations are optimized to maintain the same reactor outlet temperature at 120°C inlet temperature.

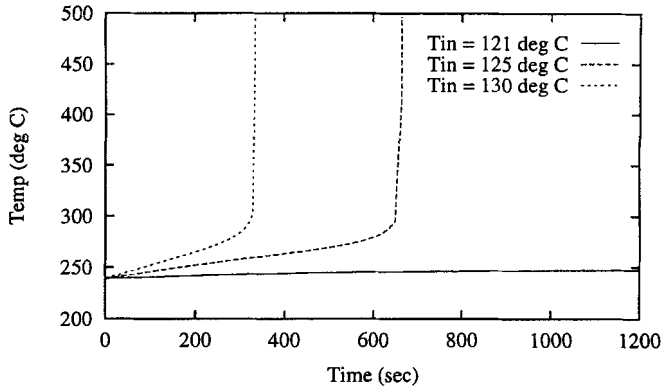

Figure 17. Influence of feed temperature disturbances.

The reactor is subjected to different feed temperature disturbances. A disturbance of 1°C changes the reactor temperature slightly, whereas disturbances of 5°C or 10°C cause a runaway.

Effects of controller

Reactor operating conditions can influence the reactor stability when subjected to a sudden feed impurity. It is typical,

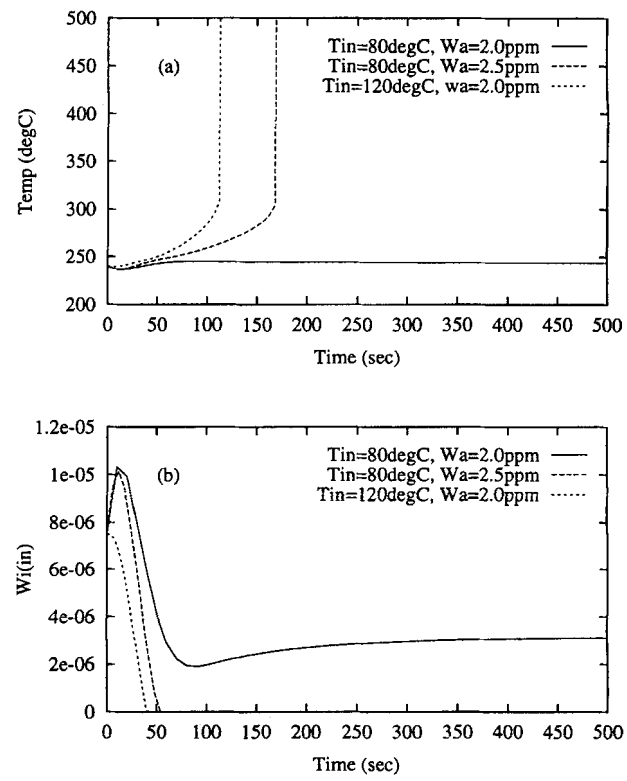

Figure 18. Influence of reactor feed temperature.

Reactors operating at two different feed temperatures are subjected to feed acetylene disturbances. A reactor with a low feed temperature can withstand a higher impurity level than a similar reactor operating with a high inlet temperature.

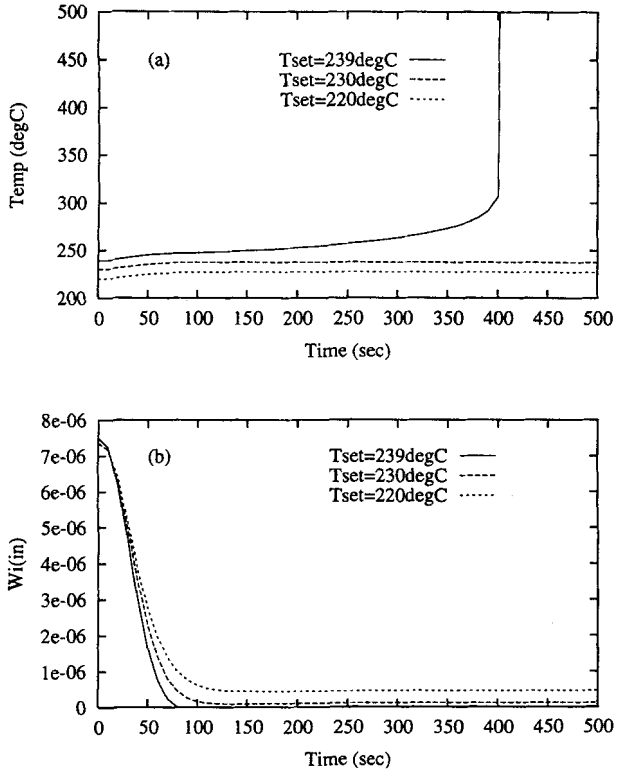

Figure 19. Effect of controller set points on the stability of the reactor.

(a) The reactor with different set points is subjected to an acetylene disturbance. (b) The responses of the manipulated variable, initiator feed, to the acetylene disturbance. The disturbance is a step increase of 1.5 ppm acetylene in the feed, and the reactor is under *P*-control.

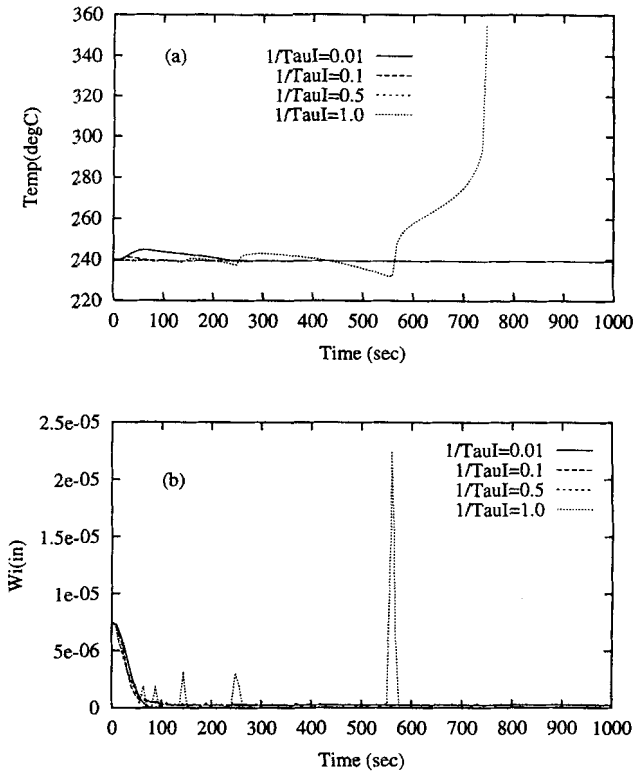

Figure 20. Effect of controller time constants on the stability of the reactor.

(a) Effect of reset time of the PI controller on reactor temperature when the reactor is subjected to 1.47 ppm acetylene disturbance. (b) The responses of the controller-manipulated variable, initiator feed, to the acetylene disturbance.

though, for these impurity disturbances to be attenuated by appropriate controller action. Figure 19 shows the effect of controller set points on the stability of the reactor subjected to impurity disturbances. When the reactor is operated at low temperature (220°C), the reactor can still achieve stable operation when there is a sudden impurity disturbance by lowering the initiator feed concentration. However, at a higher temperature set point (239°C), when the initiator feed is totally shut off, there are still radicals generated; this causes a reactor runaway.

Figure 20 shows the effect of the PI controller reset time, τ_I, on the reactor stability when the reactor is suddenly subjected to a 1.45-ppm acetylene disturbance in the feed stream. At large reset time, the controller is able to reject the impurity disturbance by lowering the initiator feed, and there is very little temperature overshoot. However, at a low τ_I value (1.0 s), the controller takes very dramatic action and finally causes a reactor runaway because the temperature becomes high enough to cause substantial monomer decomposition.

Operating strategy

During LDPE production, it is often necessary to change the reactor operating conditions to produce a different grade polymer. The reactor stability may become an important issue during this grade transition period since reactor temperature can significantly affect the polymer molecular structure and subsequently the physical properties.

A typical grade transition could be as follows. First, the reactor temperature is changed from the original 239°C to 220°C to produce a different polymer. After a certain production period at 220°C, it is desirable to bring the reactor temperature back to the original 239°C. This grade transition policy is accomplished by changing the temperature set point. There are different levels of impurity (acetylene) in the feed stream. Figure 21 shows the trajectories of the set point and reactor temperature dynamics as well as the controller-manipulated variable with different impurity levels.

When the acetylene level is at 1.3 and 1.4 ppm (mass based), the controller is able to track the desired grade transition policy with more temperature overshoot at higher impurity level (1.4 ppm). However, when the impurity level is at 1.44 ppm, the controller is able to bring the temperature down to 220°C by decreasing the initiator feed, but the reactor experiences runaway when the set point is changed back to 239°C. This situation happens because when operating at low temperature, the initiator and impurity decompose much slower and start to accumulate inside the reactor. Once the set point is changed back to the higher value, this accumulated initiator and impurity can suddenly decompose at a much higher rate and generate a large amount of free radicals, which pushes the temperature to an even higher level; at a high enough temperature, the monomer starts to decompose sig-

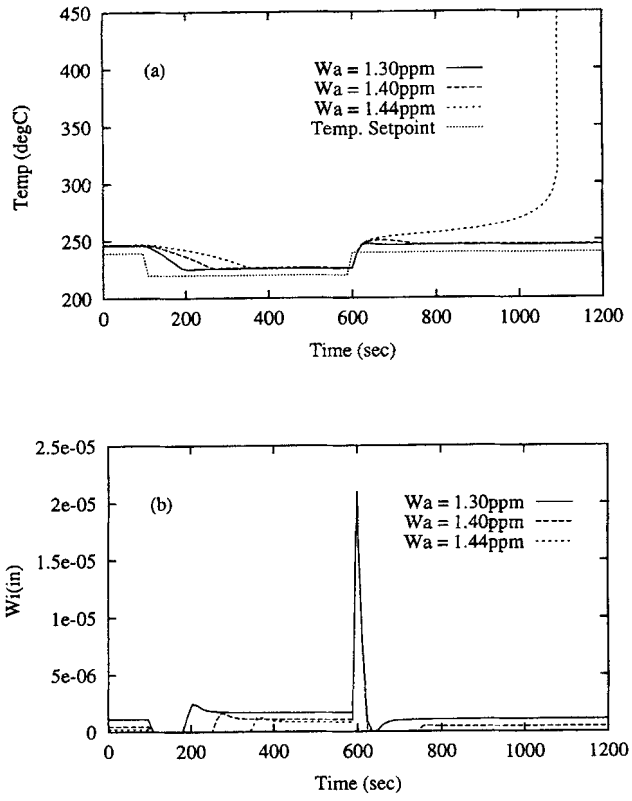

Figure 21. Effect of operating strategy.

(a) Effect of different setpoint temperature trajectories on reactor runaway. The reactor is under P control. (b) The responses of the manipulated variable, initiator feed, to the acetylene disturbance.

nificantly and the runaway ensues. The manipulated-variable, initiator feed, is totally shut off at the onset of runaway. However, this is not helpful in stopping the runaway since there is an ample amount of monomer to decompose.

Conclusions

A more general kinetic model is proposed for LDPE polymerization in an autoclave. This model not only includes the standard initiation, propagation, and termination reactions for polymerization, but it also has free radical reactions that describe the decomposition of ethylene ultimately leading to a runaway. A simplified ethylene decomposition kinetic scheme is employed, and corresponding kinetics parameters are determined from experimental observations. Dynamic simulation of the model indicates runaway behavior for the following conditions: excess initiator in feed, feed impurity, feed temperature disturbance, controller failure, and poorly tuned controller. Stability analysis indicates safe operating limits for certain variables at typical conditions. This more comprehensive model may be useful in the process design, control, and optimization of LDPE autoclaves. The present decomp model assumes the autoclave to be a perfectly mixed reactor, which is one of the limitations, since for some LDPE autoclave designs imperfect mixing exists. A subsequent article will analyze decompositions in reactors with imperfect mixing.

Acknowledgment

The authors are indebted to the National Science Foundation and the Industrial Sponsors of the University of Wisconsin Polymerization Reaction Engineering Laboratory (UWPREL) for their financial support of this research. The authors are also grateful to Dr. Robin A. Hutchinson at DuPont for helpful discussions.

Notation

c_p = total specific heat, cal·g^{-1}·°C^{-1}
C_c = centering factor of the generalized Arrhenius equation
C_j = concentration of species j, mol/L
E_a = activation energy of the generalized Arrhenius equation, cal·mol^{-1}
f = initiator decomposition efficiency
$[I]$ = initiator concentration, mol·L^{-1}
k_{d_i} = initiator i decomposition rate constant, s^{-1}
k_p = propagation rate constant, L·mol^{-1}·s^{-1}
k_{tc} = termination by combination rate constant, L·mol^{-1}·s^{-1}
k_{td} = termination by disproportionation rate constant, L·mol^{-1}·s^{-1}
k_{tsp} = spontaneous termination rate constant, L·mol^{-1}·s^{-1}
k_{tt} = total termination rate constant, L·mol^{-1}·s^{-1}
k_{tx} = termination by inhibition rate constant, L·mol^{-1}·s^{-1}
$[M]$ = monomer concentration, mol·L^{-1}
MW_i = molecular weight of monomer i, g·mol^{-1}
MW_p = average molecular weight of copolymer, g·mol^{-1}
P = reactor pressure, atm
$[P]$ = polymer concentration, mol·L^{-1}
Q_{out} = outlet volumetric flow rate, cm^3·s^{-1}
$[R]$ = free radical concentration, mol·L^{-1}
R_i = species i kinetic rate of change, mol·L^{-1}·s^{-1}
$R^k_{W_{D_i}}$ = kinetic rate of change of decomp product i, mol·L^{-1}·s^{-1}
$[S]$ = solvent concentration, mol·L^{-1}
T = temperature, °C
Temp(in) = feed temperature, °C
V = volume of reaction mixture, cm^3
V_a = activation volume of the generalized Arrhenius equation, cal/atm·mol
W_S = solvent weight fraction in the reaction mixture
W_{D_i} = weight fraction of decomp product i in the reaction mixture
X = inhibitor species
X_p = fractional conversion of monomer to polymer

Greek letters

ΔH_{decomp} = heat of ethylene decomposition, cal·mol^{-1}
ΔH_{poly} = heat of polymerization, cal·mol^{-1}
ρ_j = species j density, g·cm^3

Literature Cited

Agrawal, S. C., "Analysis of the High Pressure Polyethylene Tubular Reactor with Axial Mixing," *AIChE J.*, **21**, 449 (1975).
Arriola, D. J., *Modeling of Addition Polymerization Systems*, PhD Thesis, Univ. of Wisconsin-Madison (1989).
Beasley, J. K., "Polymerization at High Pressure," *Comprehensive Polymer Science*, S. G. Allen and J. C. Bevington, eds., Vol. 3, Pergamon Press, New York, p. 273 (1989).
Benson, S. W., and G. R. Haugen, "Mechanisms for Some High-Temperature Gas-Phase Reactions of Ethylene, Acetylene, and Butadiene," *J. Phys. Chem.*, **71**, 1735 (1967).
Bonsel, H., and G. Luft, "Safety Studies on the Explosive Degradation of Compressed Ethene," *Chem. Ing. Tech.*, **67**, 862 (1995).
Bowen, D. G., "Low-Level Ethylene Decompositions—An Inconvenience or a Warning," *Int. Symp. Loss Prevention and Safety Promotion in the Process Industries*, Vol. 1—*Safety in Operations and Processes*, Elsevier, New York, p. 1 (1983).
Brandolin, A., J. N. F. N. J. Capiati, and E. M. Vales, "Mathematical Model for High-Pressure Tubular Reactor for Ethylene Polymerization," *Ind. Eng. Chem. Res.*, **27**, 784 (1988).

Britton, L. G., D. A. Taylor, and D. C. Wobser, "Thermal Stability of Ethylene at Elevated Pressures," *Plant/Oper. Prog.*, **5**, 238 (1986).
Chan, W.-M., P. E. Gloor, and A. E. Hamielec, "A Kinetic Model for Olefin Polymerization in High Pressure Autoclave Reactors," *AIChE J.*, **39**, 111 (1993).
Chen, C. H., J. G. Vermeychuk, J. A. Howell, and P. Ehrlich, "Computer Model for Tubular High-Pressure Polyethylene Reactor," *AIChE J.*, **22**(3), 463 (1976).
Christl, R. J., and M. J. Roedel, "Constant Environment Process for Polymerizing Ethylene," U.S. Patent No. 2,897,183, to E. I. duPont de Nemours and Co. (1959).
Doak, K. W., "Low Density Polyethylene (High Pressure)," *Encyclopedia of Polymer Science and Engineering*, 2nd ed., Vol. 6, H. F. Mark, N. M. Bikales, C. G. Overberger, G. Menges, and J. I. Kroschwitz, eds., Wiley, New York, p. 386 (1986).
Doedel, E., *AUTO: Software for Continuation and Bifurcation Problems in Ordinary Differential Equations*, Tech. Rep., Caltech, Pasadena (1986).
Egloff, G., and R. E. Schaad, "Polymerisation and Explosive Decomposition of Ethylene under Pressure," *J. Inst. Pet. Technol.*, **19**, 800 (1933).
Feucht, P., B. Tilger, and G. Luft, "Prediction of Molar Mass Distribution, Number and Weight Average Degree of Polymerization and Branching of Low Density Polyethylene," *Chem. Eng. Sci.*, **40**, 1935 (1985).
Gardner, G. M., *A Theoretical Study of the Kinetics of Polyethylene Reactor Decompositions*, MS Thesis, Texas Tech Univ., Lubbock (1975).
Gay, I. G., G. B. Kistiakowsky, J. V. Michael, and H. Niki, "Thermal Decomposition of Acetylene in Shock Waves," *J. Phys. Chem.*, **43**, 1720 (1965).
Gemassmer, A. M., "Autoclave Process for the High Pressure Polymerization of Ethylene," *Erdol Kohle-Erdgas-Petrochem.*, **31**, 221 (1978).
Goto, S., K. Yamamoto, S. Furui, and M. Sugomoto, "Computer Model for Commercial High Pressure Polyethylene Reactor Based on Elementary Reaction Steps Obtained Experimentally," *J. Appl. Poly. Sci.*, **36**, 21 (1981).
Hoftyzer, P. J., and T. N. Zwietering, "The Characteristics of a Homogenized Reactor for the Polymerization of Ethylene," *Chem. Eng. Sci.*, **14**, 241 (1961).
Hollar, W., and P. Ehrlich, "An Improved Model for Temperature and Conversion Profiles in Tubular High Pressure Polyethylene Reactors," *Chem. Eng. Commun.*, **24**, 57 (1983).
Hucknall, D. J., *Chemistry of Hydrocarbon Combustion*, Chapman & Hall, London, p. 335 (1985).
Huffman, W. J., D. C. Bonner, and G. M. Gardner, "Decompositions in Polyethylene Reactors: A Theoretical Study," AIChE Meeting, Washington, DC, Paper 63d (1974).
Hyanek, I., J. Zacca, F. Teymour, and W. H. Ray, "Dynamics and Stability of Polymerization Process Flow Sheet," *Ind. Eng. Chem. Res.*, **34**, 3872 (1995).
Iwasaki, M., K. Baba, H. Ochi, S. Hirano, and T. Konaka, "Analysis of Pressure Increase Following Rapid Decomposition of Ethylene under High Pressure," *Sumitomo Kagaku (Osaka)*, **1**, 61 (1987).
Laidler, K. J., and L. F. Loucks, "The Decomposition and Isomerization of Hydrocarbons," *Comprehensive Chemical Kinetics*, Vol. 5, *Decomposition and Isomerisation of Organic Compounds*, C. H. Bamford and C. F. H. Tipper, eds., Elsevier, Amsterdam, p. 59 (1972).
Luft, G., H. Bitsch, and H. Seidl, "Effectiveness of Organic Peroxide Initiators in the High-Pressure Polymerization of Ethylene," *J. Macromol. Sci.-Chem.*, **6**, 1089 (1977).
Luft, G., and R. Neumann, "Selbstzerfall und Fremdgezundeter Zerfall von Verdichtetem Athylen," *Chem. Ing. Tech.*, **50**, 620 (1978).
Marini, L., and C. Georgakis, "Low-Density Polyethylene Vessel Reactors Part I: Steady State and Dynamic Modelling," *AIChE J.*, **30**, 401 (1984a).
Marini, L., and C. Georgakis, "The Effect of Imperfect Mixing on Polymer Quality in Low Density Polyethylene Vessel Reactor," *Chem. Eng. Commun.*, **30**, 361 (1984b).
Martinot, B., "Reduction of Explosion Risks Subsequent to Ethylene Decomposition on High Pressure Polyethylene Plants," *The Protection of Exothermic Reactors and Pressurized Storage Vessels*, Pergamon Press, New York, p. 315 (1984).
Mavridis, H., and C. Kiparissides, "Optimization of a High Pressure Polyethylene Tubular Reactor," *Poly. Process. Eng.*, **3**(3), 263 (1985).
McKay, F. F., G. R. Worrell, B. C. Thornton, and H. L. Lewis, "If an Ethylene Pipe Line Ruptures...," *Hydroc. Process.*, **56**, 487 (1977).
Miller, S. A., "Biological Properties and Other Chemical Properties," *Ethylene and Its Industrial Derivatives*, S. A. Miller, ed., Ernest Benn, London, p. 1118 (1969).
Neumann, R., and G. Luft, "Untersuchungen Zum Thermischen Zerfall von Aethylen unter Hochdruck," *Chem. Eng. Sci.*, **28**, 1505 (1973).
Petzold, L. R., *A Description of DASSL: A Differential-Algebraic System Solver*, Tech. Rep. SAND82-8637, Sandia National Laboratories Report (1982).
Scott, G. S., R. E. Kennedy, I. Spolan, and M. G. Zabetakis, *Flammability Characteristics of Ethylene*, Tech. Rep. 6659, Bureau of Mines, Boulder, CO (1965).
Shirodkar, P. P., and G. O. Tsien, "A Mathematical Model for the Production of Low Density Polyethylene in a Tubular Reactor," *Chem. Eng. Sci.*, **41**(4), 1031 (1986).
Sullivan, J. F., and D. I. Shannon, "Decomposition Venting in a Polyethylene Product Separator," *Codes and Standards and Applications for High Pressure Equipment*, J. E. Staffiera, ed., ASME, New York, p. 191 (1992).
Tanzawa, T., and W. C. Gardiner, "Reaction Mechanism of the Homogeneous Thermal Decomposition of Acetylene," *J. Phys. Chem.*, **84**, 236 (1980).
Tomura, Y., H. Nagashima, and K. Shirayama, "New Process for LD-PE," *Hydroc. Proc.*, **57**, 151 (1978).
Towell, G. D., and J. J. Martin, "Kinetic Data from Nonisothermal Experiments: Thermal Decomposition of Ethane, Ethylene, and Acetylene," *AIChE J.*, **7**, 693 (1961).
Verros, G., M. Papadakis, and C. Kiparissides, "Mathematical Modelling of High Pressure Tubular LDPE Copolymerization Reactors," *Poly. React. Eng.*, **1**(3), 427 (1993).
Watanabe, H., K. Kurihara, and M. Takehisa, "The Explosive Decomposition of Ethylene," *Proc. Pacific Chemical Engineering Congress (PACHEC)*, AIChE, New York, p. 225 (1972).
Waterman, H. I., and A. J. Tulleners, "Decomposition of Ethylene by Heating under High Pressure," *J. Inst. Pet. Technol.*, **17**, 506 (1931).
Worrell, G. R., "If An Ethylene Decomposes in Pipe...," *Hydroc. Process.*, **58**, 255 (1979).
Zabisky, R. C. M., W. M. Chan, P. E. Gloor, and A. E. Hamielec, "A Kinetic Model for Olefin Polymerization in High-Pressure Tubular Reactors," *Polymer*, **33**, 2243 (1992).
Zacca, J., X. Zhang, and W. H. Ray, "Reactor Runaway Phenomena in Polymerization Processes," *Int. Symp. Runaway Reaction and Pressure Relief Design*, H. Fisher, ed., AIChE, New York (1995).
Zimmermann, T., and G. Luft, "Untersuchungen Zum Explosiven Zerfall von Verdichtetem Ethylen," *Chem. Ing. Tech.*, **66**, 1386 (1994).

Manuscript received Dec. 4, 1995, and revision received Feb. 22, 1996.